THE JOURNAL OF BIOLOGICAL CHEMISTRY Vol. 279, No. 5, Issue of January 30, pp. 3151–3159, 2004
Printed in U.S.A.

Roles of TRP14, a Thioredoxin-related Protein in Tumor Necrosis Factor-α Signaling Pathways*

Received for publication, July 22, 2003, and in revised form, October 15, 2003
Published, JBC Papers in Press, November 7, 2003, DOI 10.1074/jbc.M307959200

Woojin Jeong‡§, Tong-Shin Chang‡§, Emily S. Boja¶, Henry M. Fales¶, and Sue Goo Rhee‡‖

From the ‡Laboratory of Cell Signaling, NHLBI, National Institutes of Health, Bethesda, Maryland 20892, the §Center for Cell Signaling Research, Ewha Womans University, Seoul 120-750, Korea, and the ¶Laboratory of Biophysical Chemistry, NHLBI, National Institutes of Health, Bethesda, Maryland 20892

The possible roles of a 14-kDa human thioredoxin (Trx)-related protein (TRP14) in TNF-α signaling were studied in comparison with those of Trx1 by RNA interference in HeLa cells. Depletion of TRP14 augmented the TNF-α-induced phosphorylation and degradation of IκBα as well as the consequent activation of NF-κB to a greater extent than did Trx1 depletion. Deficiency of TRP14 or Trx1 enhanced TNF-α-induced activation of caspases and subsequent apoptosis by a similar extent. The TNF-α-induced activation of c-Jun N-terminal kinase (JNK) and p38 mitogen-activated protein kinases (MAPKs), however, was promoted by depletion of TRP14 but not by that of Trx1. Unlike Trx1, TRP14 neither associated with nor inhibited the kinase activity of apoptosis signal-regulating kinase-1 (ASK1), an upstream activator of JNK and p38. In combination with the results in the accompanying paper that TRP14 did not reduce the known substrates of Trx1, these results suggest that TRP14 modulates TNF-α signaling pathways, provably by interacting with proteins distinct from the targets of Trx1. In an effort to identify target proteins of TRP14, a mutant of TRP14, in which the active site cysteine (Cys^{46}) was substituted with serine, was shown to form a disulfide-linked complex with LC8 cytoplasmic dynein light chain. The complex was detected in HeLa cells treated with H_2O_2 or TNF-α but not in untreated cells, suggesting that LC8 cytoplasmic dynein light chain is a possible substrate of TRP14.

The cellular redox state is affected not only by normal respiration and metabolism but also by the transient production of reactive oxygen species (ROS)[1] that results from the ligation of various cell surface receptors (1–3). Tumor necrosis factor-α (TNF-α) was one of the first receptor ligands shown to generate ROS in nonphagocytic cells and is among the ligands whose signaling pathways have been studied most in relation to ROS production (4, 5). The binding of TNF-α to TNF receptor 1 (TNFR1) generates both proapoptotic and prosurvival signals by inducing the formation of a multiprotein signaling complex at the cell membrane. This complex in turn triggers the caspase cascade, the activation of specific kinases such as the IκB kinase (IKK) complex and mitogen-activated protein kinases (MAPKs), and the transcription of various genes mediated by nuclear factor-κB (NF-κB) and activator protein-1 (AP-1) (6–10). Many TNF-α signaling pathways are activated by ROS (7, 11–16) and attenuated by Trx overexpression (17–25).

In the accompanying study (26), we identified and characterized a 14-kDa cytosolic protein, designated Trx-related protein 14 (TRP14). Here we studied the possible roles of TRP14 in TNF-α signaling in comparison with those of Trx1 by RNA interference (RNAi) in HeLa cells. Partial depletion of TRP14 or Trx1 by RNAi resulted in enhancement of TNF-α-induced activation of caspases and NF-κB. The TNF-α-induced activation of c-Jun-N-terminal kinase (JNK) and p38 MAPK, however, was augmented by depletion of TRP14 but not by that of Trx1. Furthermore, unlike Trx1, reduced TRP14 neither bound to nor inhibited the activity of apoptosis signal-regulating kinase 1 (ASK1), a MAPKKK that activates JNK and p38 pathways. These results suggest that TNF-α signaling pathways are modulated differentially by TRP14 and Trx1 in response to changes in cellular redox state.

It was previously shown that Trx substrates could be trapped using a mutant Trx, in which the C-terminal active site cysteine was substituted with serine (27, 28). A similar procedure was applied here to identify LC8 cytoplasmic dynein light chain as a possible target of TRP14.

EXPERIMENTAL PROCEDURES

Materials—Goat antibody to human Trx1 was obtained from American Diagnostica; mouse monoclonal antibodies (mAbs) to poly (ADP-ribose) polymerase (PARP) and to LC8 were from BD Biosciences; rabbit antibodies to phosphorylated IκBα, to phosphorylated JNK, to phosphorylated p38 MAPK, to caspase-3, and to caspase-9 as well as a mAb to caspase-8 were from Cell Signaling Technology; rabbit antibodies to IκBα, to JNK1, and to Bid were from Santa Cruz Biotechnology; a mAb to β-actin was from Abcam; rabbit antibodies to Mn^{2+}-dependent superoxide dismutase (MnSOD) were from Upstate Biotechnology; and mAbs to the FLAG epitope and to the hemagglutinin epitope (HA) were from Sigma and Roche Applied Science, respectively. Agarose beads conjugated with anti-HA were from Santa Cruz Biotechnology. The fluorogenic caspase substrates DEVD-AMC and LEHD-AMC were from BD Pharmingen and Biomol, respectively. The pcDNA3-ASK1-FLAG and GST-SEK1 (KR) were from H. Ichijo (Graduate School of Pharmaceutical Sciences, Tokyo University) and L. Zon (Howard Hughes Medical Institute, Harvard Medical School), respectively. Mammalian expression vectors, pCR-TRP14 and pHA-TRP14 were constructed by inserting human TRP14 cDNA into the EcoRI and XhoI sites of pCR3.1

* This work was supported in part by the Korean Science and Engineering Foundation Center of Excellence grant to the Center for Cell signaling Research at Ewha Womans University (to W. J. and T.-S. C.). The costs of publication of this article were defrayed in part by the payment of page charges. This article must therefore be hereby marked "*advertisement*" in accordance with 18 U.S.C. Section 1734 solely to indicate this fact.

‖ To whom correspondence should be addressed: Bldg. 50, Room 3523, South Drive, MSC 8015, Bethesda, MD 20892. Tel.: 301-496-9646; Fax: 301-480-0357; E-mail: sgrhee@nih.gov.

[1] The abbreviations used are: ROS, reactive oxygen species; TNF-α, tumor necrosis factor-α; TNFR1, TNF receptor 1; IKK, IκB kinase; MAPK, mitogen-activated protein kinase; NF-κB, nuclear factor-κB; Trx, thioredoxin; TRP14, 14-kDa thioredoxin-related protein; RNAi, RNA interference; JNK, c-Jun NH_2-terminal kinase; ASK1, apoptosis signal-regulating kinase 1; mAb, monoclonal antibody; PARP, poly (ADP-ribose) polymerase; LC-MS/MS, reversed-phase HPLC coupled with tandem mass spectrometry; MnSOD, Mn^{2+}-dependent superoxide dismutase; siRNA, small interfering RNA; DTT, dithiothreitol; GST, glutathione *S*-transferase; CHAPS, 3-[(3-cholamidopropyl)dimethylammonio]-1-propanesulfonic acid.

(Invitrogen) and the XbaI and BamHI sites of pCGN vector (W. Herr, Cold Spring Harbor laboratory), respectively. To express HA-tagged Trx1 in HeLa cells, pHA-Trx1 was constructed by cloning human Trx1 gene at the XbaI and BamHI sites of pCGN vector. For the production of GST-TRP14 protein, DNA sequence encoding TRP14 was cloned into the EcoRI and XhoI sites of pGEX4T1 vector. Vectors for expression of C-terminal cysteine mutant TRP14, pGST-TRP14-C46S and pHA-TRP14-C46S were generated by site-directed mutagenesis using QuickChange kit (Stratagene). To express FLAG-tagged LC8 in HeLa cells, pFLAG-LC8 was constructed by cloning the human LC8 gene at the HindIII and EcoRI sites of pFLAG-CMV2 vector (Sigma).

Immunoblot Analysis—Cellular total proteins (20 μg, unless indicated otherwise) were fractionated by sodium dodecyl sulfate-polyacrylamide gel electrophoresis (SDS-PAGE) and then transferred to a nitrocellulose membrane. The membrane was incubated at room temperature for 1 h first with 5% dried nonfat milk in TBST (20 mM Tris-HCl (pH 7.5), 150 mM NaCl, 0.1% Tween 20) and then with primary antibodies in the same solution. After washing of the membrane with TBST, immune complexes were detected with horseradish peroxidase-conjugated secondary antibodies and enhanced chemiluminescence reagents (PerkinElmer Life Sciences).

Depletion of TRP14 or Trx1 by RNAi—Small interfering RNAs (siRNAs) that target human TRP14 and human Trx1 mRNAs were based on nucleotides 104–122 and 256–276, respectively, relative to the translation start site. The siRNAs were synthesized with T7 RNA polymerase (29) and introduced into HeLa cells as described (30). In brief, the cells were harvested by exposure to trypsin, diluted with fresh medium without antibiotics, and transferred to 6-well plates. After incubation for 24 h, the cells were transfected with the siRNAs for 2.5 days with the use of OligofectAMINE (Invitrogen). The Scramble II Duplex (Dharmacon) served as a negative control for siRNA activity. A mixture of 12 μl of OptiMEM medium (Invitrogen) and 3 μl of OligofectAMINE was incubated for 10 min at room temperature and was then combined with 10 μl of 20 μM siRNA diluted with 175 μl of OptiMEM. The resulting mixture (200 μl) was incubated for 20 min at room temperature to allow complex formation and then overlaid onto each well containing the cells for a final volume of 1.5 ml per well.

Flow Cytometry—Cells ($\sim 1 \times 10^6$) were washed twice with ice-cold phosphate-buffered saline, fixed overnight at 4 °C in 70% ethanol, resuspended in 400 μl of a solution containing propidium iodide (25 μg/ml), DNase-free RNase (10 μg/ml), and 0.1% Nonidet P-40, and incubated for 1 h at room temperature. Cell cycle analysis was then performed with a FACSCalibur flow cytometer (BD Biosciences). A total of 25,000 nuclei were analyzed for each sample, and the cell cycle distribution was quantified with WinMDI software.

Immune Complex Kinase Assay—HeLa cells were subjected to transient transfection in 100-mm dishes with 4 μg of pcDNA3-ASK1-FLAG and 12 μl of FuGENE 6 transfection reagent (Roche Applied Science). After 24 h, the cells were exposed to 1 mM H_2O_2 for 20 min, washed twice with ice-cold phosphate-buffered saline, and then lysed for 10 min at 4 °C in a solution containing 25 mM HEPES-NaOH (pH 7.4), 2 mM EGTA, 25 mM β-glycerophosphate, 1% Triton X-100, 10% glycerol, 1 mM Na_3VO_4, 5 mM NaF, 1 mM 4-(2-aminoethyl)benzene-sulfonyl fluoride, aprotinin (10 μg/ml), leupeptin (10 μg/ml), and 25 nM microcystin. The lysates (1 mg of protein) were then incubated for 2 h at 4 °C with 15 μl of Anti-FLAG M2 affinity gel (Sigma) with constant rotation. The resulting immune complexes were washed twice with cell lysis buffer and twice with washing buffer (20 mM HEPES-NaOH, pH 7.0, 100 mM $MgCl_2$, 1 mM dithiothreitol (DTT)) before use as the source of ASK1. The phosphorylation of 1 μg of a GST-SEK1(KR) was performed for 30 min at 30 °C with immunoprecipitated ASK1-FLAG in a final volume of 40 μl containing 20 mM HEPES-NaOH (pH 7.0), 1 mM DTT, 1 mM Na_3VO_4, 100 mM $MgCl_2$, 100 μM ATP, and 10 μCi of [γ-^{32}P]ATP in the absence or presence of the indicated concentrations of recombinant TRP14 or Trx1 pretreated with 1 mM DTT. The reaction mixture was then subjected to SDS-PAGE, and the radioactivity associated with the GST-SEK1(KR) band was quantified by PhosphorImager (Molecular Dynamics) analysis.

LC-MS/MS Analysis of Protein Digests—Protein bands stained with Coomassie Blue were excised, reduced, and alkylated, followed by trypsinization as previously described (31). These digests were then analyzed on a Micromass QTOF Ultima Global (Micromass, Manchester, UK) in electrospray mode interfaced with an Agilent HP1100 CapLC (Agilent Technologies, Palo Alto, CA) prior to the mass spectrometer. 5 μl of each digest was loaded onto a Vydec C_{18} MS column (100 × 0.15 mm; Grace Vydec, Hesperia, CA) and chromatographic separation was performed at 1 μl/min using the following gradient: 0–10% B over 5 min; gradient from 10–40% B over 60 min; 40–95% B over 5 min; 95% B held over 5 min (solvent A: 0.2% formic acid in water; solvent B: 0.2% formic acid in acetonitrile). A data-dependent analysis (DDA) method collected CID data for the three most abundant multiply charged ions observed in the preceding survey scan (*m/z* 300–1990) above a threshold of 10 counts/sec. Data was processed using the MassLynx (version 3.5) to generate peak list files before submitting them to Mascot search at www.matrixscience.com (MatrixScience Ltd., London, UK).

RESULTS

Roles of TRP14 and Trx1 in TNF-α-induced NF-κB Activation—TNF-α is a potent stimulator of NF-κB activation. It has been shown that ROS generally augments the NF-κB activation (7, 11–16), whereas overexpression of redox-regulatory molecules such as Trx suppresses it (22, 23, 32). We therefore examined the effect of overexpression of TRP14 on TNF-α-induced NF-κB activation in HeLa cells that had also been transfected with an NF-κB-dependent luciferase reporter gene. Transient overexpression of TRP14 resulted in a dose-dependent inhibition of the TNF-α-induced increase in reporter gene activity (Fig. 1*A*).

The role of endogenous Trx1 in the TNF-α-induced activation of NF-κB was also previously examined by introducing Trx1-specific antisense oligonucleotides into HeLa cells. The substantial depletion of Trx1 induced by these oligonucleotides was not accompanied by a corresponding increase in NF-κB-dependent luciferase reporter gene expression, however (23). We applied RNAi to reduce the abundance of endogenous TRP14 or Trx1 in HeLa cells and then monitored expression of the endogenous MnSOD gene, which is induced in response to NF-κB activation (33–35). Two and half days after transfection of cells with the corresponding siRNA, the abundance of TRP14 and Trx1 was reduced by ~70 and ~90%, respectively, compared with the values for cells transfected with a control RNA (Fig. 1*B*). This partial depletion of TRP14 resulted in an increase in MnSOD expression of about 2-fold in unstimulated cells and of ~1.7-fold in TNF-α-stimulated cells (Fig. 1*B*). The depletion of Trx1 also increased MnSOD expression by about 2-fold in unstimulated cells but only by ~1.2-fold in TNF-α-stimulated cells (Fig. 1*B*). These results thus indicated that TRP14 is a more potent inhibitor of NF-κB activity than is Trx1 in HeLa cells.

In response to activating signals such as TNF-α, the inhibitory protein IκB, which binds to NF-κB and sequesters it in the cytoplasm under resting conditions, is phosphorylated and subsequently degraded by the ubiquitin-proteasome system, thereby allowing NF-κB to translocate to the nucleus and to activate gene expression (6, 8). Overexpression of Trx1 was previously shown to inhibit TNF-α-induced degradation of IκBα in HeLa cells (23). We therefore examined the effects of TRP14 or Trx1 depletion on the time course of IκBα phosphorylation and degradation (Fig. 1*C*). Transfection of cells with the TRP14 siRNA increased the rate and extent of serine phosphorylation of IκBα, compared with those apparent in cells transfected with control RNA, and these effects were accompanied by an increase in the rate of IκBα degradation. Transfection with the Trx1 siRNA also enhanced the TNF-α-induced phosphorylation and degradation of IκBα, but to a lesser degree than did that with the TRP14 siRNA. These results are thus consistent with those showing that TRP14 depletion had a greater effect on TNF-α-induced MnSOD expression than did Trx1 depletion.

Roles of TRP14 and Trx1 in TNF-α-induced Apoptosis and Caspase Activation—Exposure of cells to TNF-α triggers the activation of a caspase cascade that leads to apoptosis (6, 7). However, TNF-α also activates two transcription factors, AP-1 and NF-κB, that induce the expression of genes that act to suppress TNF-α-induced apoptosis, explaining why the apoptotic response to TNF-α usually depends on inhibition of pro-

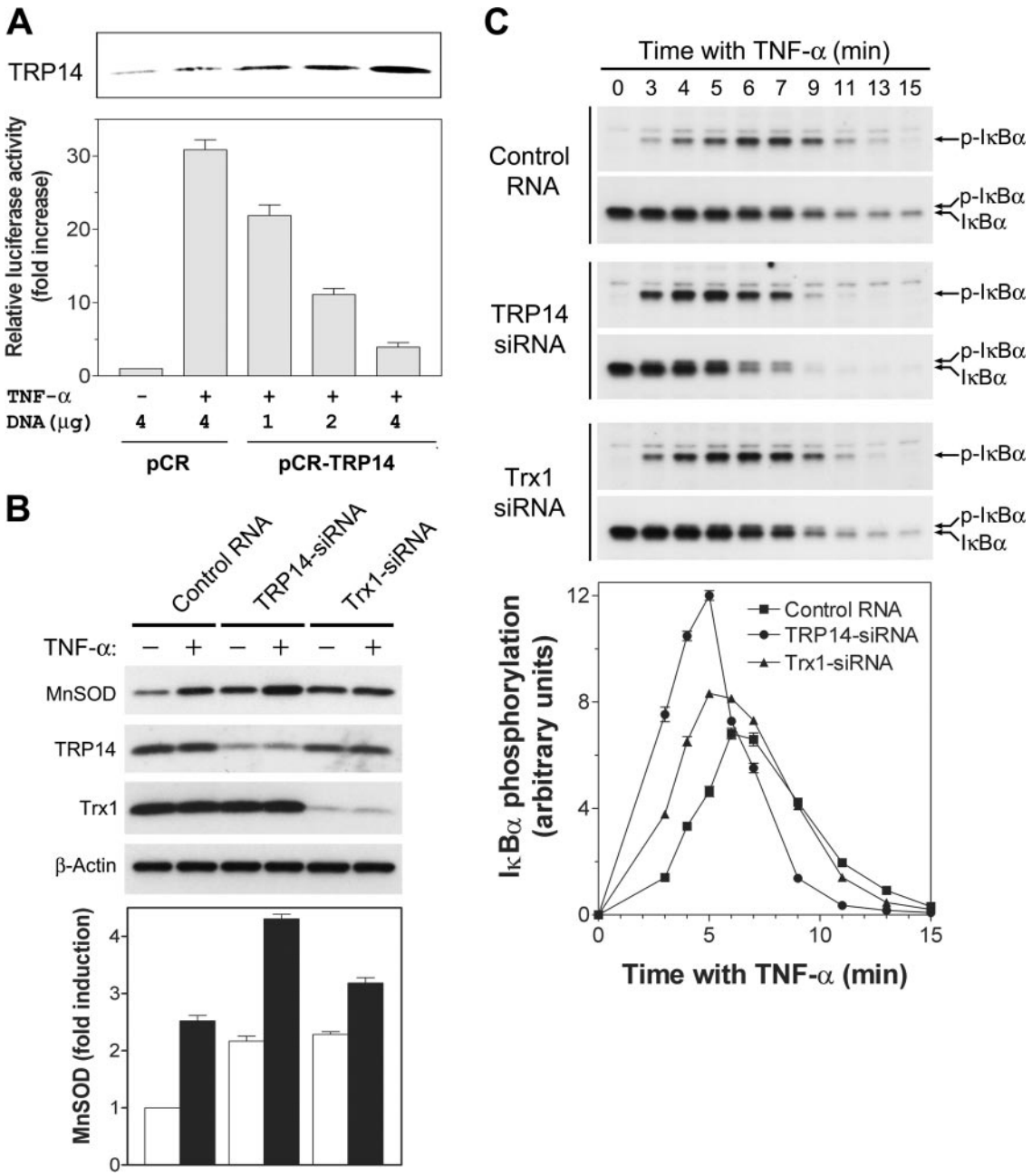

FIG. 1. **Modulation of TNF-α-induced NF-κB activation by TRP14 and Trx1.** *A*, effect of TRP14 overexpression on NF-κB activation. HeLa cells were cotransfected for 24 h with 4 μg of pCR or the indicated amounts of pCR-TRP14, 0.5 μg of pNF-κB-Luc (NF-κB reporter plasmid; Stratagene), and 0.5 μg of pRL-SV40 (internal control). The total amount of plasmid DNA was adjusted to 5 μg with pCR vector. The cells were then incubated in the absence or presence of TNF-α (20 ng/ml) for 4 h, after which the abundance of TRP14 was determined by immunoblot analysis of cell lysates with anti-TRP14 (*upper panel*). The luciferase activities of cell lysates were also measured with a dual-luciferase assay system. The activity of firefly luciferase was normalized by that of the *Renilla* enzyme and was then expressed as fold increase relative to the activity of pCR-transfected cells (*lower panel*). Data are means ± S.E. of values from three independent experiments. *B*, effect of depletion of TRP14 or Trx1 on NF-κB activation. HeLa cells were transfected for 2.5 days with a control RNA, TRP14 siRNA, or Trx1 siRNA and then incubated in the absence or presence of TNF-α (15 ng/ml) for 6 h. The abundance of MnSOD, TRP14, Trx1, and β-actin in cell lysates was then determined by immunoblot analysis (*upper panels*). The chemiluminescence signal for MnSOD was quantified with a Kodak Image Station and ImageQuant software and was normalized by that for β-actin (*lower panel*). Data are means ± S.E. of values from three independent experiments. *C*, effect of TRP14 or Trx1 depletion on serine phosphorylation and degradation of IκBα. HeLa cells were transfected with control RNA, TRP14 siRNA, or Trx1 siRNA for 2.5 days and then stimulated with TNF-α (15 ng/ml) for the indicated times. Cell lysates were then subjected to immunoblot analysis with antibodies to phospho-IκBα or to IκBα (upper and lower of each pair of images, respectively). The chemiluminescence signals for phospho-IκBα were quantified and normalized (*lower panel*) as in *B*.

tein synthesis (36). Although several studies have addressed the issue, the role of Trx1 in apoptosis induced by oxidants or other agents remains unclear (37–39). We examined the effect of TRP14 or Trx1 depletion on TNF-α-induced apoptosis in HeLa cells in which protein synthesis was blocked by cycloheximide. Transfection of cells with TRP14 or Trx1 siRNAs increased the number of dead cells as revealed by phase-contrast microscopy both 4 and 8 h after exposure to TNF-α and cycloheximide (Fig. 2*A*). We also quantified apoptotic cells by flow cytometry after staining with propidium iodide. The number of apoptotic cells (those with a subdiploid (<2N) DNA content) at various times after exposure to TNF-α and cycloheximide was increased by a factor of 2–3 by partial depletion of TRP14 or Trx1 (Fig. 2, *B* and *C*).

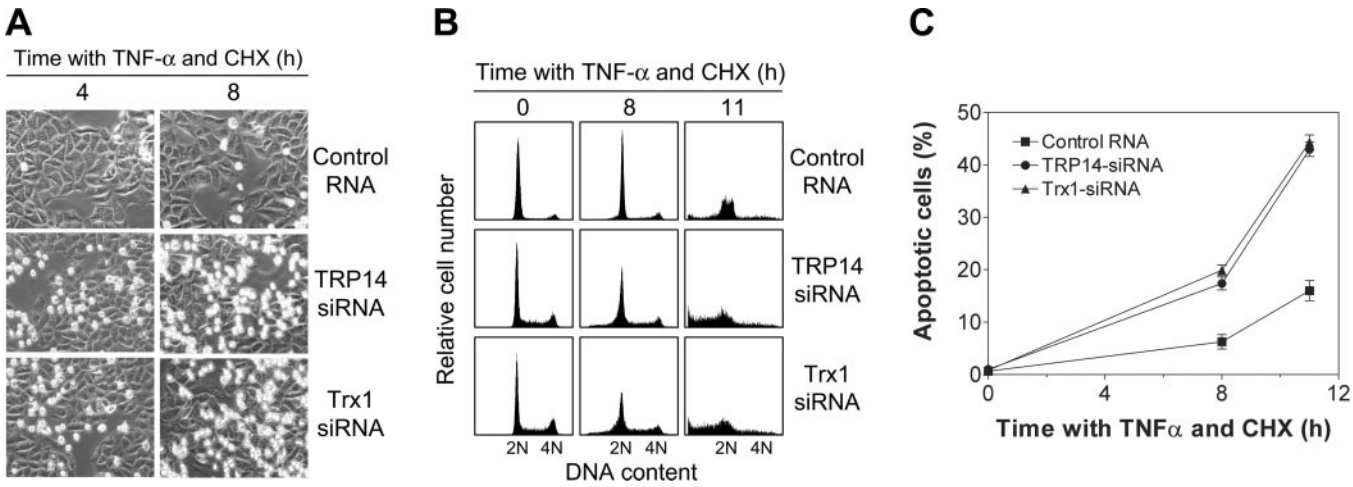

FIG. 2. **Effects of partial depletion of TRP14 or Trx1 on TNF-α-induced apoptosis in HeLa cells.** *A*, cells were transfected with control RNA, TRP14 siRNA, or Trx1 siRNA for 2.5 days and then incubated with both TNF-α (15 ng/ml) and cycloheximide (10 μg/ml) for 4 or 8 h. The cells were then examined by phase-contrast microscopy (original magnification, ×20). *B* and *C*, cells were transfected and incubated for the indicated times with TNF-α and cycloheximide as in *A*, stained with propidium iodide, and subjected to flow cytometric analysis of DNA content (*B*). The percentage of apoptotic cells was determined as the percentage of cells with a DNA content of <2N (*C*). Data in *C* are means ± S.E. of values from three independent experiments.

A critical event in TNF-α-induced apoptosis is the activation of caspase-8 (6, 40, 41). Active caspase-8 then cleaves other procaspases to initiate a caspase cascade (42) as well as cytosolic Bid to generate a truncated form of this protein; the latter translocates to mitochondria and induces the release of cytochrome *c*, which triggers the activation of caspase-9 (43). Both of these signaling pathways triggered by caspase-8 converge on caspase-3, the active form of which mediates the degradation of many apoptotic substrates including PARP (44). We examined the effect of TRP14 or Trx1 depletion on the time courses of the TNF-α-induced cleavage of procaspases-8, -9, and -3, Bid, and PARP by immunoblot analysis (Fig. 3, *A* and *B*). Depletion of either TRP14 or Trx1 accelerated the cleavage of all five proteins. The cleavage of procaspase-8 and that of PARP, which correspond to the most upstream and downstream events, were affected least and most, respectively, by depletion of TRP14 or Trx1. The effects of TRP14 or Trx1 deficiency on caspase-3 and caspase-9 activation were confirmed by measurement of the corresponding protease activities with specific fluorogenic substrates (Fig. 3*C*).

Roles of TRP14 and Trx1 in TNF-α-induced Activation of JNK and p38 MAPK—TNF-α also induces the activation of various MAPKs, most notably JNK and p38 (6, 36, 45, 46). Ectopic expression of Trx1 was previously shown to inhibit the TNF-α-induced activation of JNK and p38 (19, 24). We therefore examined whether the TNF-α-induced activation of these MAPKs in HeLa cells was affected by transfection with TRP14 or Trx1 siRNAs. MAPKs are activated by dual phosphorylation of threonine and tyrosine residues (Thr^{183} and Tyr^{185} for JNK; Thr^{180} and Tyr^{182} for p38) within a T*X*Y motif (47). Immunoblot analysis with antibodies specific for the dually phosphorylated proteins revealed that, although the time courses of TNF-α-induced JNK and p38 phosphorylation in TRP14-deficient cells were similar to those in control cells, the extent of phosphorylation of both proteins was increased by a factor of ~2 in the TRP14-deficient cells (Fig. 4). In contrast, the time course and extent of JNK and p38 phosphorylation were unaffected by Trx1 depletion.

TRP14 Neither Associates with Nor Inhibits the Activity of ASK1—Reduced Trx1 binds to and inhibits the activity of ASK1, a MAPK kinase kinase that phosphorylates and activates MAPK kinases that in turn activate JNK and p38 by phosphorylating their T*X*Y motifs (18, 19, 48). To examine whether TRP14 also associates with ASK1, we transfected HeLa cells with expression vectors for FLAG-tagged ASK1 and either HA-tagged TRP14 or HA-tagged Trx1. Immunoblot analysis of immunoprecipitates prepared from cell lysates with antibodies to HA revealed that ASK1-FLAG coprecipitated with HA-Trx1 but not with HA-TRP14 (Fig. 5*A*). We also examined the effects of TRP14 and Trx1 on the kinase activity of immunoprecipitated ASK1-FLAG with a GST-SEK1 fusion protein as substrate. SEK1 (also known as MKK4) is a MAPK kinase that is phosphorylated by ASK1. TRP14 at concentrations up to 6 μM did not affect the activity of ASK1-FLAG, whereas this activity was markedly inhibited by Trx1 at similar concentrations (Fig. 5*B*). Thus, unlike Trx1, TRP14 does not appear to interact with ASK1.

LC8 Is a Possible Target Protein of TRP14—During the reduction process of substrate, Trx forms a mixed disulfide intermediate with the substrate using its N-terminal cysteine of the C*XX*C motif (Cys^{32} in human Trx1). Given that the release of substrate from the disulfide-linked intermediate requires an attack of the disulfide by the C-terminal cysteine of the C*XX*C motif (Cys^{35} in human Trx1), the intermediate can be stabilized when Trx lacks the C-terminal Cys as seen previously with plant Trx (27, 28).

To identify possible target proteins of TRP14, we produced a GST-fusion protein (GST-TRP14-C46S) of mutant TRP14, in which the C-terminal C*XX*C motif cysteine (Cys^{46}) was substituted with serine, and immobilized the fusion proteins on glutathione (GSH) resins. HeLa cell lysate that had been subjected to air oxidation was incubated with the resin to allow the formation of the mixed-disulfide intermediate. The proteins bound to the resin were eluted by incubation with a buffer containing 10 mM DTT and subjected to SDS-PAGE. A resin prepared using the GST fusion protein (GST-TRP14) of wild type TRP14 was used as a control. When protein bands eluted from the mutant resin were compared with those from the control resin, selective retention by the mutant resin of three proteins of 8, 13, and 20 kDa was apparent (Fig. 6*A*). Individual bands were identified by slicing out the protein bands, in gel trypsinization, followed by LC-MS/MS. As shown in Table I, the 8 kDa protein was identified as LC8 dynein light chain (LC8) also known as Dlc-1 (dyenin light chain 1) or PIN (protein inhibitor of neuronal nitric-oxide synthase); the 20 kDa protein as cofilin; and the 13 kDa protein as ribosomal protein L30.

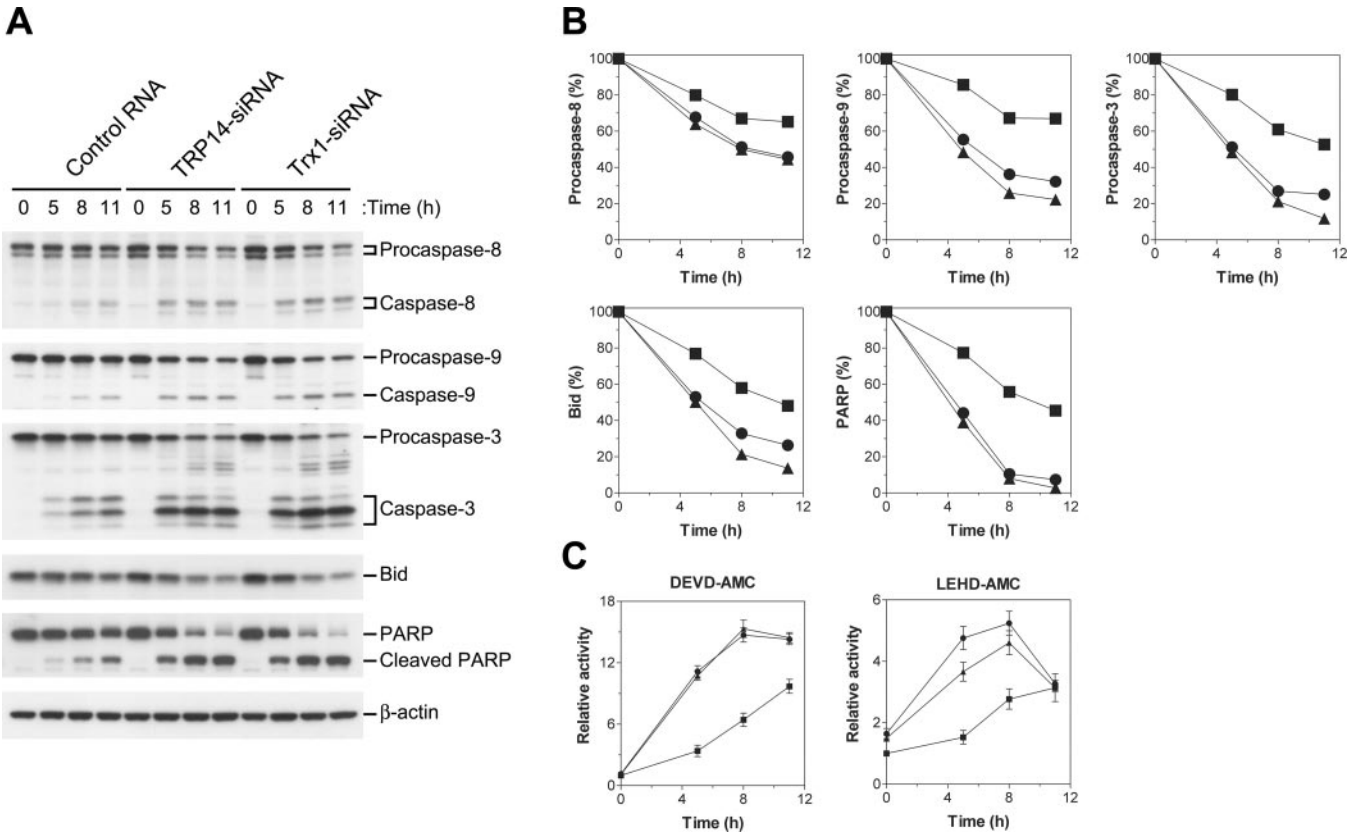

FIG. 3. **Effects of TRP14 or Trx1 deficiency on TNF-α-induced caspase activation in HeLa cells.** Cells were transfected with control RNA, TRP14 siRNA, or Trx1 siRNA for 2.5 days and then incubated for the indicated times with TNF-α (15 ng/ml) and cycloheximide (10 μg/ml). *A* and *B*, cell lysates were then subjected to immunoblot analysis with antibodies to caspase-8, to caspase-9, to caspase-3, to Bid, to PARP, or to β-actin (*Control*). The bands corresponding to the uncleaved proteins in *A* were scanned with a Personal Densitometer SI (Molecular Dynamics) and quantified by ImageQuant (version 5.2) software. The data were normalized by the amount of β-actin, and expressed as a percentage of the value for time 0 (■, control RNA; ●, TRP14-siRNA; ▲, Trx1-siRNA). Similar results were obtained in three independent experiments. *C*, the same cell lysates (10 μg of protein) were assayed for the activities of caspase-3 and caspase-9 by incubation at 37 °C in a reaction mixture (200 μl) containing 100 mM HEPES-KOH (pH 7.5), 10% (w/v) sucrose, 0.1% CHAPS detergent, 10 mM DTT, and 25 μM fluorogenic substrate (DEVD-AMC and LEHD-AMC, respectively). The amount of fluorescent aminomethylcoumarin (*AMC*) liberated was measured with a CytoFluor 4000 instrument (PerSeptive Biosystems) at excitation and emission wavelengths of 380 and 460 nm, respectively. Data are expressed as relative activities compared with those of cells that were transfected with control RNA and not exposed to TNF-α and cycloheximide (■, control RNA; ●, TRP14-siRNA; ▲, Trx1-siRNA). They are means ± S.D. of triplicates from an experiment that was repeated twice with similar results.

Identity of the 8 and 20 kDa proteins was confirmed by immunoblot analyses with anti-LC8 and anti-cofilin antibodies, respectively (Fig. 6*B*).

There is convincing data supporting a physical association of LC8 with the NF-κB inhibitor IκBα (49) and with the Bcl-2 family member Bim (50). Thus, we examined whether TRP14 does form the mixed-disulfide intermediate with LC8 in cells. We transiently expressed FLAG-LC8 together with HA-TRP14 or HA-TRP14-C46S in HeLa cells and isolated the TRP14-LC8 complex by immunoprecipitation with anti-FLAG antibody. In cells grown under a normal condition, neither HA-TRP14 nor HA-TRP14-C46S formed a complex with FLAG-LC8 (Fig. 7, *left panels*). When the cells treated with H_2O_2 or TNF-α, however, LC8 formed mixed-disulfide intermediate with HA-TRP14-C46S but not with HA-TRP14-WT (Fig. 7, *center* and *right panels*). These results indicate that in oxidatively stressed cells LC8 forms a disulfide, which is the target of reduction by TRP14. Similar trapping experiments in cells were not carried out for cofilin or ribosomal protein L30.

DISCUSSION

Exposure of cells to TNF-α induces the production of ROS by a mechanism that remains largely unknown (7). These ROS alter the cellular redox potential and mediate various aspects of TNF-α-induced signaling (7, 11–16). Trx1 has been shown to counteract the effects of ROS in TNF-α signaling (22, 23, 32), mostly on the basis of results obtained with cells overexpressing Trx1, given that targeted disruption of the mouse Trx1 gene resulted in early embryonic death (51). We have now evaluated the cellular functions of TRP14 in the context of TNF-α signaling and in comparison with those of Trx1 by RNAi in HeLa cells. The amount of TRP14 in HeLa cells is about one-sixth that of Trx1 (0.3 and 1.8 μg per milligram of lysate protein, respectively) (see accompanying article, Ref. 26), and transfection of the cells with the respective siRNA reduced the abundance of TRP14 by ~70% and that of Trx1 by ~90%.

The TNF-α-induced activation of NF-κB is mediated by the phosphorylation and subsequent degradation of IκB proteins (7, 36). Degradation of IκB allows NF-κB to translocate to the nucleus and to activate the transcription of its target genes. The binding of NF-κB to DNA requires that a specific cysteine residue of its p50 subunit be in the reduced state. NF-κB was one of the first transcription factors shown to be activated by ROS (5). Although ROS were initially proposed to be central mediators of NF-κB activation (7), this role depends both on cell type and on cell status (11, 52–55). In some cell types, NF-κB activity is actually inhibited by exposure to H_2O_2 (54). Furthermore, IκB phosphorylation, ubiquitination, and degradation in the cytosol as well as NF-κB phosphorylation and binding to DNA in the nucleus have each been shown to be affected by H_2O_2 (54). These observations indicate that the TNF-α signal-

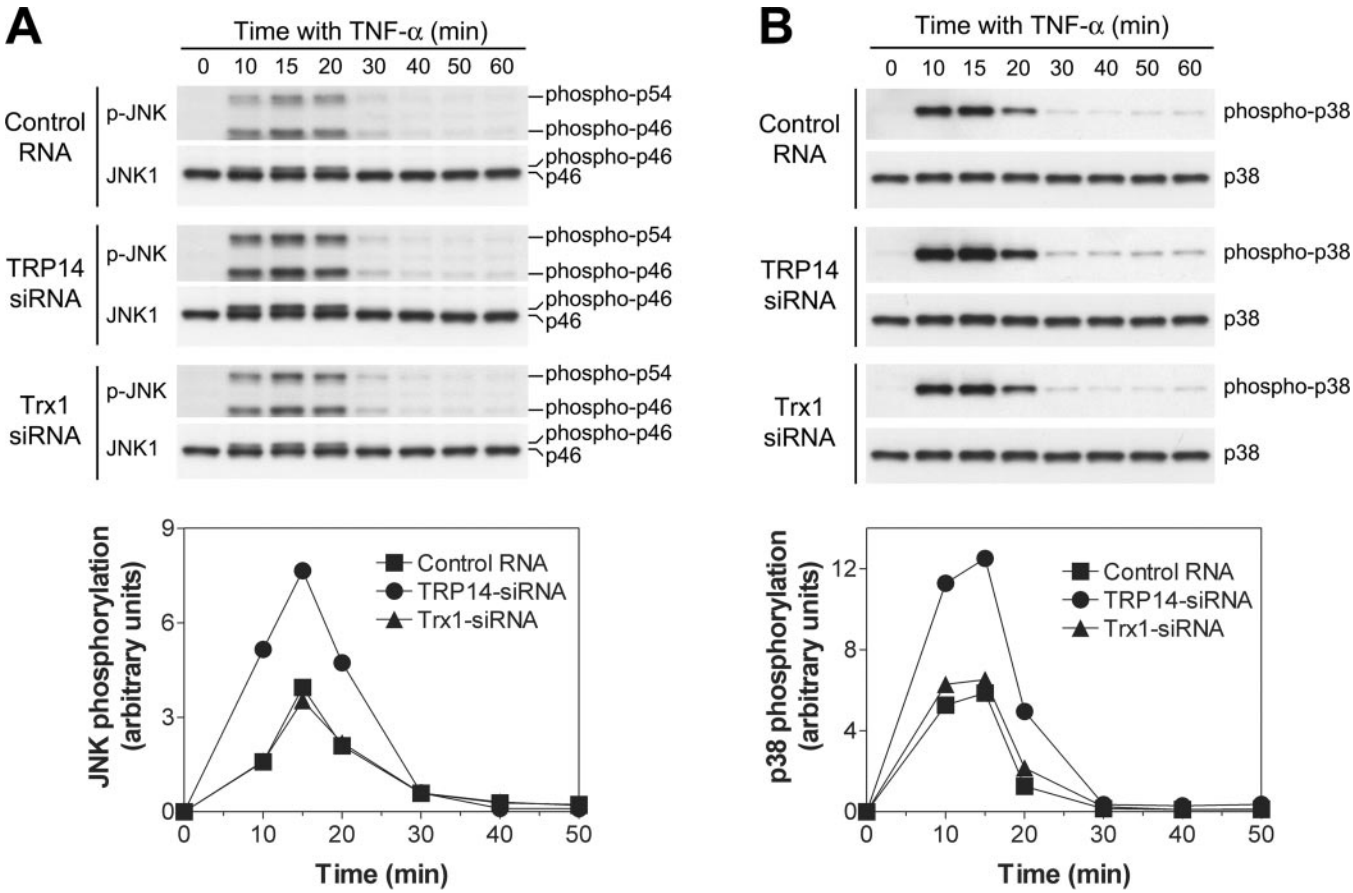

FIG. 4. **Effects of partial depletion of TRP14 or Trx1 on TNF-α-induced phosphorylation of JNK (*A*) and p38 MAPK (*B*).** HeLa cells were transfected with control RNA, TRP14 siRNA, or Trx1 siRNA for 2.5 days and then incubated for the indicated times with TNF-α (15 ng/ml). Cell lysates were then subjected to immunoblot analysis with antibodies to phospho-JNK or to phospho-p38; the membranes were also reprobed with antibodies to JNK1 or to p38, respectively. The signals corresponding to phospho-JNK (p54 and p46 isoforms) and to phospho-p38 were scanned and quantitated as described in the legend to Fig. 1*A*. The data were normalized by the amount of β-actin. Similar results were obtained in a total of three independent experiments.

ing pathway leading to NF-κB activation might be affected at various steps by regulatory proteins with redox-sensitive cysteines and probably requires C*XX*C-containing proteins to reduce the oxidized forms of these regulatory proteins.

Trx1 has been suggested to play distinct roles in the cytoplasm and in the nucleus with regard to regulation of NF-κB-dependent transcription. In the cytoplasm, Trx1 suppresses the degradation of IκB. In the nucleus, Trx1 is thought to associate physically with and to reduce a disulfide of NF-κB, thereby promoting transactivation (23, 32, 56, 57). However, the final outcome of Trx1 overexpression in HeLa cells was inhibition, not activation, of NF-κB-dependent gene expression (23).

We have now shown that TRP14 overexpression inhibited the TNF-α-induced transcription of an NF-κB reporter gene (Fig. 1*A*). The partial depletion of TRP14 or Trx1 by RNAi resulted in enhancement of NF-κB activity in both unstimulated and TNF-α-stimulated cells as indicated by increased expression of MnSOD, the product of an NF-κB target gene (Fig. 1*B*). The enhancement of NF-κB-dependent gene expression was associated with increased phosphorylation and degradation of IκBα (Fig. 1*C*). TRP14 appears to be more potent than Trx1 as a modulator of the NF-κB signaling pathway: Although HeLa cells contain less TRP14 than Trx1, and RNAi was less effective for TRP14 than for Trx1, both MnSOD expression as well as the phosphorylation and degradation of IκBα were affected to a greater extent by TRP14 siRNA than by TrxR1 siRNA (Fig. 1, *B* and *C*). The final outcome with regard to NF-κB-dependent gene expression was moderate activation after 90% depletion of Trx1, which was also associated with a slight enhancement of IκBα phosphorylation and degradation. This observation suggests that the inhibitory role of Trx1 in the cytoplasm is more important than its stimulatory role in the nucleus, probably because the redox status of NF-κB is regulated predominantly by other nuclear-resident C*XX*C proteins such as nucleoredoxin (Nrx) and glutaredoxin (Grx) (58).

The partial depletion of TRP14 or Trx1 promoted TNF-α-induced apoptosis (Fig. 2) and this effect was accompanied by accelerated activation of caspases-8, -9, and -3 as well as increased degradation of the caspase substrates Bid and PARP (Fig. 3). TNF-α-induced apoptosis is initiated by the recruitment by Fas-associated death domain (FADD) of procaspase-8 to the TNFR1 receptor complex, which results in the autocleavage and activation of this enzyme (7, 36). Caspase-8, in turn, triggers two separate signaling pathways, one of which is mediated by mitochondria and results in the activation of caspase-9 and both of which converge on caspase-3. ROS also induce caspase activation and apoptosis (7, 59). Caspase activation, however, is not a direct effect of ROS because all caspases are cysteine proteases and require the active site cysteine in the reduced state (60). Purified caspases are inactivated by peroxides, and prolonged and excessive oxidative stress prevents caspase activation in cells (59). Overexpression of Trx was previously shown to inhibit TNF-α-induced caspase activation and apoptosis (25). It is possible that these effects of Trx are mediated in part through inhibition of the activation of ASK1 induced by TNF-α. Expression of kinase-inactive ASK1 mutants inhibited oxidant- or TNF-α-induced apoptosis (61), whereas a

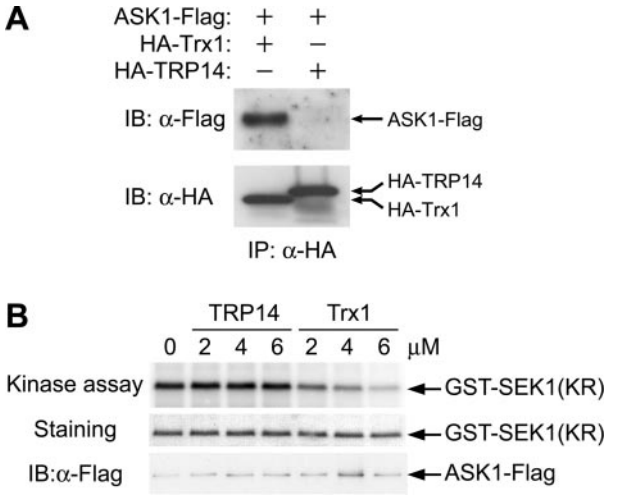

FIG. 5. **Interaction of ASK1 with Trx1 but not with TRP14.** *A*, HeLa cells in 100-mm dishes were cotransfected for 24 h with 3 μg of pcDNA3-ASK1-FLAG and 3 μg of either pHA-Trx1 or pHA-TRP14, after which the cells were lysed in 1 ml of a solution containing 20 mM Tris-HCl (pH 7.5), 1 mM EDTA, 150 mM NaCl, 1% Triton X-100, 1 mM 4-(2-aminoethyl)benzene-sulfonyl fluoride, aprotinin (10 μg/ml), and leupeptin (10 μg/ml). The lysates were then subjected to immunoprecipitation (*IP*) for 2 h at 4 °C with 20 μl of agarose beads conjugated with anti-HA, and the resulting precipitates were washed three times with lysis buffer and then subjected to immunoblot analysis (*IB*) with anti-FLAG or anti-HA. *B*, HeLa cells were transfected with pcDNA3-ASK1-FLAG for 24 h and then exposed to 1 mM H_2O_2 for 20 min. Cell lysates were then subjected to immunoprecipitation with anti-FLAG, and the resulting precipitates were assayed for kinase activity with GST-SEK1(KR) as substrate in the presence of the indicated concentrations of TRP14 or Trx1 (see under "Experimental Procedures"). The assay gel was also stained with Coomassie Blue and subjected to immunoblot analysis with anti-FLAG, as indicated.

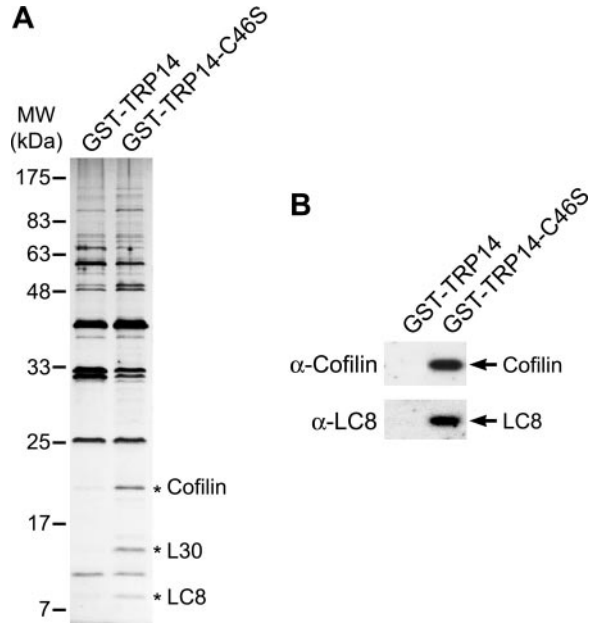

FIG. 6. **Identification of LC8 as a possible target protein of TRP14.** *A*, TRP14-immobilized resins were prepared by incubating purified GST-TRP14 or GST-TRP14-C46S (8 mg) with GSH-Sepharose resin (1 ml) according to the manufacturer's instructions. HeLa cells were lysed by sonication in a buffer containing 50 mM Tris-HCl (pH 8.0), 150 mM NaCl, 1 mM EDTA, 1 mM 4-(2-aminoethyl)benzene-sulfonyl fluoride, leupeptin (10 μg/ml), and apoprotinin (10 μg/ml), and the clarified lysate was stored at 4 °C overnight to allow air-oxidation. The cell lysate (50 mg) was then incubated with 0.5 ml of the TRP14-WT- or TRP14-C46S-immobilzed resins at room temperature for 1h. After washing the resins with the lysis buffer until the A_{280} of the eluant became almost zero, proteins were eluted by incubating the resins with the lysis buffer containing 10 mM DTT for 30 min at room temperature. The eluted proteins were separated on 14% SDS-acrylamide gel and visualized by Coomassie brilliant blue R-250. Three bands selectively eluted from the TRP14-C46S resin were indicated by *asterisk*. *B*, immunoblot analysis of the eluted samples using anti-cofilin and anti-LC8 antibodies.

constitutively active mutant of ASK1 induced mitochondrial-dependent caspase activation (activation of caspases-9 and -3 but not -8) (62). Furthermore, ASK1-deficient cells are resistant to TNF-α-induced apoptosis (63). However, inhibition of ASK1 cannot explain the effect of Trx1 on the mitochondria-independent activation of caspase-8. It is also possible that Trx overexpression results in an increased scavenging of peroxides by Trx-dependent peroxiredoxin (Prx) activity. Given that TRP14 neither inhibits ASK1 (Fig. 5*B*) nor activates Prx, its effects on apoptosis and caspase activation appear to be mediated through targets distinct from those of Trx1.

The TNFR1-associated TRAF2 induces the activation of several MAPK kinase kinases, each of which is able to activate JNK and p38 (36, 64). ASK1 is one such MAPK kinase kinase and is also a target of the sensor and transducer function of Trx1. Overexpression of Trx1 was previously shown to inhibit ASK1 activity, resulting in suppression of ROS- or TNF-α-induced activation of JNK and p38 in HEK293 cells (18, 19). Partial depletion of Trx1 with antisense oligonucleotides also increased ASK1 activity in these cells (18). We have now demonstrated an interaction between ectopically expressed Trx1 and ASK1 in HeLa cells (Fig. 5*A*). However, depletion of Trx1 in HeLa cells did not result in a detectable increase in the extent of JNK or p38 activation induced by TNF-α (Fig. 4), suggesting that the pathways linking TNFR1 to the activation of JNK and p38 are dependent on cell type and context. It is also possible that ASK1 is not a critical MAPK kinase kinase for the activation of JNK or p38, as suggested by the observation that ASK1-deficient fibroblasts exhibited normal JNK and p38 activation during the early phase of TNF-α engagement and manifested only a partial defect in sustained kinase activation (63). In contrast to Trx1, partial depletion of TRP14 resulted in marked enhancement of the activation of JNK and p38 by TNF-α (Fig. 4). Given that TRP14 does not interact with ASK1 (Fig. 5*A*), the TNF-α-induced activation of JNK and p38 likely involves other proteins that are targets for the disulfide reductase activity or redox-transducer function of TRP14.

Our present data showed that TRP14 is a previously unidentified modulator of TNF-α signaling pathways. Although TRP14 is less abundant than Trx1 in HeLa cells, the effects of partial depletion of TRP14 on the TNF-α-induced activation of NF-κB, JNK, and p38 were more pronounced than those of Trx1 depletion, whereas TRP14 and Trx1 deficiency affected TNF-α-induced apoptosis by similar extents. Given that all TNF-α signaling pathways are initiated by the same upstream receptor complex and are tightly linked through a sophisticated network of cross-talk, it is not clear whether each of the pathways includes distinct TRP14 targets. Its biochemical properties predict that TRP14 is a disulfide reductase like Trx1. However, TRP14 failed to reduce several known Trx1 substrates (26), suggesting that disulfide reductases such as TRP14 and Trx1 might interact with their respective substrates with a higher degree of specificity than previously appreciated.

Using a substrate trapping method that had been successfully applied to identify Trx target proteins in plant cells (27, 28), we picked up LC8, cofilin, and ribosomal protein L30 as potential substrates of TRP14 (Fig. 6). LC8 is likely a physiological substrate of TRP14 as it formed a disulfide-linked complex with TRP14 in oxidatively stressed cells. LC8, a compo-

TABLE I
LC-MS/MS of tryptic digests of three protein bands

Bands	Protein identified	*m/z* observed[a] (monoisotopic)	Δ mass	Residues	Sequence from database
			Da		
20 kDa	Cofilin (83% coverage)	377.23^{2+}	0.08	14–19	VFNDMK
		512.81^{2+}	0.09	14–21	VFNDM*KVP[b]
		502.81^{2+}	0.09	23–30	SSTPEEVKK
		566.85^{2+}	0.07	22–31	KSSTPEEVKK
		591.33^{2+}	0.07	35–44	AVLFC*LSEDK[c]
		655.36^{2+}	0.03	35–45	AVLFC*LSEDKK
		766.38^{4+}	−0.09	46–73	NIILEEGKEILVGDVGQTVDDPYATFVK
		517.78^{2+}	0.08	74–81	MLPDKDC*R
		669.32^{2+}	0.01	82–92	YALYDATYETK
		664.04^{3+}	0.04	96–112	KEDLVFIFWAPESAPLK
		400.25^{2+}	0.10	115–121	MIYASSK
		330.27^{2+}	0.08	127–132	KLTGIK
		597.64^{3+}	0.08	133–146	HELQANC*YEEVKDR
		670.91^{2+}	0.03	153–166	LGGSAVISLEGKPL
13 kDa	60 S ribosomal protein L30 (36% coverage)	453.29^{2+}	0.10	10–17	SLESINSR
		371.76^{2+}	0.10	27–32	YVLGYK
		677.41^{2+}	0.04	45–56	LVILANNC*PALR
		879.41^{2+}	−0.09	91–106	VC*TLAIIDPGDSDIIR
8 kDa	LC8/PIN (64% coverage)	975.71^{3+}	−0.21	6–31	AVIKNADMSEEMQQDSVEC*ATQALEK
		849.31^{3+}	−0.11	10–31	NADM*SEEM*QQDSVEC*ATQALEK
		333.72^{2+}	0.09	32–36	YNIEK
		472.31^{3+}	0.14	32–43	YNIEKDIAAHIK
		384.27^{2+}	0.10	37–43	DIAAHIK
		448.32^{2+}	0.10	37–44	DIAAHIKK
		397.77^{2+}	0.10	44–49	KEFDKK
		468.27^{3+}	0.14	50–60	YNPTWHC*IVGR

[a] Indicates the charge state of each m/z observed.
[b] M* is methionine sulfoxide generated during sample preparation.
[c] C* represents carbamidomethylated cysteine.

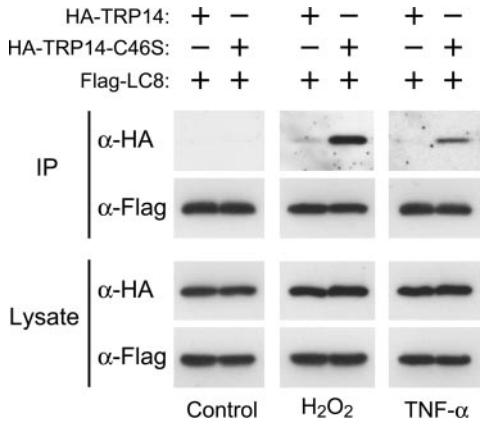

FIG. 7. **Detection of LC8-TRP14-C46S complex in HeLa cells.** HeLa cells in 60-mm dishes were cotransfected for 24 h with 1.8 μg of pFLAG-LC8 and 0.2 μg of either pHA-TRP14 or pHA-TRP14-C46S and then were exposed to either 500 μM H_2O_2 or TNF-α (20 ng/ml) for 1h. The cells were lysed as described in the legend to Fig. 5, the lysates were incubated with anti-FLAG M2 monoclonal antibody (20 μg) for 1 h at 4 °C, and the immune complexes were precipitated with G-Sepharose. After washing three times with the lysis buffer, the immunoprecipitated proteins (*IP*) were subjected to immunoblot analysis with anti-HA (α-HA) or anti-FLAG (α-FLAG) antibodies. The lysates (*Lysate*) were also subjected to the same immunoblot analysis to check the expression of HA-tagged and FLAG-tagged proteins.

nent of cytoplasmic dynein complex (65, 66), acts as a multifunctional regulatory protein. LC8 (PIN) is known to bind to and inhibit neuronal nitric-oxide synthase (67). Importantly, LC8 (Dcl-1) physically interacts with the N-terminal regulatory domain of IκBα, suggesting its potential role in the activation of NFκB (49). Furthermore, LC8 tightly binds to the Bcl-2 family member Bim, and this binding sequesters the majority of Bims to the microtubule-associated dynein complex (50). Thus, LC8 is likely an intermediary molecule that links the reductase activity of TRP14 to NFκB activation as well as to apoptosis in TNF-α-stimulated cells. Substantiation of the roles of LC8 and TRP14 in the TNF-α signaling pathways obviously demands many more studies, including those addressing the TNF-α-dependent change in the redox state of LC8.

Acknowledgments—We thank H. Ichijo for pcDNA3-ASK1-FLAG, L. Zon for GST-SEK1(KR), and W. Herr for pCGN vector.

REFERENCES

1. Rhee, S. G. (1999) *Exp. Mol. Med.* **31,** 53–59
2. Rhee, S. G., Bae, Y. S., Lee, S.-R., and Kwon, J. (2000) *Science's Stke* http://www.stke.org/cgi/content/full/OC_sigtrans;2000/53/pe1
3. Finkel, T. (1998) *Curr. Opin. Cell Biol.* **10,** 248–253
4. Meier, B., Radeke, H. H., Selle, S., Younes, M., Sies, H., Resch, K., and Habermehl, G. G. (1989) *Biochem. J.* **263,** 539–545
5. Schreck, R., Rieber, P., and Baeuerle, P. A. (1991) *EMBO J.* **10,** 2247–2258
6. Chen, G., and Goeddel, D. V. (2002) *Science* **296,** 1634–1635
7. Garg, A. K., and Aggarwal, B. B. (2002) *Mol. Immunol.* **39,** 509–517
8. Ghosh, S., and Karin, M. (2002) *Cell* **109** (suppl.)**,** S81–96
9. Baeuerle, P. A., and Baltimore, D. (1996) *Cell* **87,** 13–20
10. Davis, R. J. (2000) *Cell* **103,** 239–252
11. Li, N., and Karin, M. (1999) *Faseb J.* **13,** 1137–1143
12. Schulze-Osthoff, K., Bakker, A. C., Vanhaesebroeck, B., Beyaert, R., Jacob, W. A., and Fiers, W. (1992) *J. Biol. Chem.* **267,** 5317–5323
13. Shoji, Y., Uedono, Y., Ishikura, H., Takeyama, N., and Tanaka, T. (1995) *Immunology* **84,** 543–548
14. Goossens, V., Grooten, J., De Vos, K., and Fiers, W. (1995) *Proc. Natl. Acad. Sci. U. S. A.* **92,** 8115–8119
15. Mehlen, P., Kretz-Remy, C., Preville, X., and Arrigo, A. P. (1996) *EMBO J.* **15,** 2695–2706
16. Fernandez-Checa, J. C., Kaplowitz, N., Garcia-Ruiz, C., Colell, A., Miranda, M., Mari, M., Ardite, E., and Morales, A. (1997) *Am. J. Physiol.* **273,** G7–17
17. Matsuda, M., Masutani, H., Nakamura, H., Miyajima, S., Yamauchi, A., Yonehara, S., Uchida, A., Irimajiri, K., Horiuchi, A., and Yodoi, J. (1991) *J. Immunol.* **147,** 3837–3841
18. Saitoh, M., Nishitoh, H., Fujii, M., Takeda, K., Tobiume, K., Sawada, Y., Kawabata, M., Miyazono, K., and Ichijo, H. (1998) *EMBO J.* **17,** 2596–2606
19. Liu, H., Nishitoh, H., Ichijo, H., and Kyriakis, J. M. (2000) *Mol. Cell. Biol.* **20,** 2198–2208
20. Liu, Y., and Min, W. (2002) *Circ. Res.* **90,** 1259–1266
21. Song, J. J., Rhee, J. G., Suntharalingam, M., Walsh, S. A., Spitz, D. R., and Lee, Y. J. (2002) *J. Biol. Chem.* **277,** 46566–46575
22. Takeuchi, J., Hirota, K., Itoh, T., Shinkura, R., Kitada, K., Yodoi, J., Namba, T., and Fukuda, K. (2000) *Antioxid. Redox Signal* **2,** 83–92
23. Hirota, K., Murata, M., Sachi, Y., Nakamura, H., Takeuchi, J., Mori, K., and Yodoi, J. (1999) *J. Biol. Chem.* **274,** 27891–27897
24. Hashimoto, S., Matsumoto, K., Gon, Y., Furuichi, S., Maruoka, S., Takeshita, I., Hirota, K., Yodoi, J., and Horie, T. (1999) *Biochem. Biophys. Res. Commun.* **258,** 443–447

25. Ueda, S., Masutani, H., Nakamura, H., Tanaka, T., Ueno, M., and Yodoi, J. (2002) *Antioxid. Redox Signal* **4,** 405–414
26. Jeong, W., Yoon, H. W., Lee, S.-R., and Rhee, S. G. (2004) *J. Biol. Chem.* **279,** 3142–3150
27. Verdoucq, L., Vignols, F., Jacquot, J. P., Chartier, Y., and Meyer, Y. (1999) *J. Biol. Chem.* **274,** 19714–19722
28. Motohashi, K., Kondoh, A., Stumpp, M. T., and Hisabori, T. (2001) *Proc. Natl. Acad. Sci. U. S. A.* **98,** 11224–11229
29. Donze, O., and Picard, D. (2002) *Nucleic Acids Res.* **30,** e46
30. Chang, T. S., Jeong, W., Choi, S. Y., Yu, S., Kang, S. W., and Rhee, S. G. (2002) *J. Biol. Chem.* **277,** 25370–25376
31. Ihling, C., Berger, K., Hofliger, M. M., Fuhrer, D., Beck-Sickinger, A. G., and Sinz, A. (2003) *Rapid Commun. Mass Spectrom.* **17,** *1240–1246*
32. Schenk, H., Klein, M., Erdbrugger, W., Droge, W., and Schulze-Osthoff, K. (1994) *Proc. Natl. Acad. Sci. U. S. A.* **91,** 1672–1676
33. Xu, Y., Kiningham, K. K., Devalaraja, M. N., Yeh, C. C., Majima, H., Kasarskis, E. J., and St Clair, D. K. (1999) *DNA Cell Biol.* **18,** 709–722
34. Wan, X. S., Devalaraja, M. N., and St Clair, D. K. (1994) *DNA Cell Biol.* **13,** 1127–1136
35. Wong, G. H. (1995) *Biochim. Biophys. Acta* **1271,** 205–209
36. Baud, V., and Karin, M. (2001) *Trends Cell Biol.* **11,** 372–377
37. Ma, X., Karra, S., Lindner, D. J., Hu, J., Reddy, S. P., Kimchi, A., Yodoi, J., Kalvakolanu, D. V., and Kalvakolanu, D. D. (2001) *Oncogene* **20,** 3703–3715
38. Andoh, T., Chock, P. B., and Chiueh, C. C. (2002) *J. Biol. Chem.* **277,** 9655–9660
39. Baker, A., Santos, B. D., and Powis, G. (2000) *Biochem. Biophys. Res. Commun.* **268,** 78–81
40. Sartorius, U., Schmitz, I., and Krammer, P. H. (2001) *Chembiochem.* **2,** 20–29
41. Medema, J. P., Scaffidi, C., Kischkel, F. C., Shevchenko, A., Mann, M., Krammer, P. H., and Peter, M. E. (1997) *EMBO J.* **16,** 2794–2804
42. Chang, H. Y., and Yang, X. (2000) *Microbiol. Mol. Biol. Rev.* **64,** 821–846
43. Wang, X. (2001) *Genes Dev.* **15,** 2922–2933
44. Casciola-Rosen, L., Nicholson, D. W., Chong, T., Rowan, K. R., Thornberry, N. A., Miller, D. K., and Rosen, A. (1996) *J. Exp. Med.* **183,** 1957–1964
45. Natoli, G., Costanzo, A., Ianni, A., Templeton, D. J., Woodgett, J. R., Balsano, C., and Levrero, M. (1997) *Science* **275,** 200–203
46. Liu, Z. G., Hsu, H., Goeddel, D. V., and Karin, M. (1996) *Cell* **87,** 565–576
47. Payne, D. M., Rossomando, A. J., Martino, P., Erickson, A. K., Her, J. H., Shabanowitz, J., Hunt, D. F., Weber, M. J., and Sturgill, T. W. (1991) *EMBO J.* **10,** 885–892
48. Matsuzawa, A., Nishitoh, H., Tobiume, K., Takeda, K., and Ichijo, H. (2002) *Antioxid. Redox Signal* **4,** 415–425
49. Crepieux, P., Kwon, H., Leclerc, N., Spencer, W., Richard, S., Lin, R., and Hiscott, J. (1997) *Mol. Cell. Biol.* **17,** 7375–7385
50. Puthalakath, H., Huang, D. C., O'Reilly, L. A., King, S. M., and Strasser, A. (1999) *Mol. Cell* **3,** 287–296
51. Matsui, M., Oshima, M., Oshima, H., Takaku, K., Maruyama, T., Yodoi, J., and Taketo, M. M. (1996) *Dev. Biol.* **178,** 179–185
52. Bowie, A., and O'Neill, L. A. (2000) *Biochem. Pharmacol.* **59,** 13–23
53. Bonizzi, G., Piette, J., Merville, M. P., and Bours, V. (2000) *Biochem. Pharmacol.* **59,** 7–11
54. Korn, S. H., Wouters, E. F., Vos, N., and Janssen-Heininger, Y. M. (2001) *J. Biol. Chem.* **276,** 35693–35700
55. Jaspers, I., Zhang, W., Fraser, A., Samet, J. M., and Reed, W. (2001) *Am. J. Respir. Cell Mol. Biol.* **24,** 769–777
56. Toledano, M. B., and Leonard, W. J. (1991) *Proc. Natl. Acad. Sci. U. S. A.* **88,** 4328–4332
57. Qin, J., Yang, Y., Velyvis, A., and Gronenborn, A. (2000) *Antioxid. Redox Signal* **2,** 827–840
58. Hirota, K., Matsui, M., Murata, M., Takashima, Y., Cheng, F. S., Itoh, T., Fukuda, K., and Yodoi, J. (2000) *Biochem. Biophys. Res. Commun.* **274,** 177–182
59. Hampton, M. B., Fadeel, B., and Orrenius, S. (1998) *Ann. N. Y. Acad. Sci.* **854,** 328–335
60. Wilson, K. P., Black, J. A., Thomson, J. A., Kim, E. E., Griffith, J. P., Navia, M. A., Murcko, M. A., Chambers, S. P., Aldape, R. A., Raybuck, S. A. *et al.* (1994) *Nature* **370,** 270–275
61. Ichijo, H., Nishida, E., Irie, K., ten Dijke, P., Saitoh, M., Moriguchi, T., Takagi, M., Matsumoto, K., Miyazono, K., and Gotoh, Y. (1997) *Science* **275,** 90–94
62. Hatai, T., Matsuzawa, A., Inoshita, S., Mochida, Y., Kuroda, T., Sakamaki, K., Kuida, K., Yonehara, S., Ichijo, H., and Takeda, K. (2000) *J. Biol. Chem.* **275,** 26576–26581
63. Tobiume, K., Matsuzawa, A., Takahashi, T., Nishitoh, H., Morita, K., Takeda, K., Minowa, O., Miyazono, K., Noda, T., and Ichijo, H. (2001) *EMBO Rep.* **2,** 222–228
64. Tournier, C., Dong, C., Turner, T. K., Jones, S. N., Flavell, R. A., and Davis, R. J. (2001) *Genes Dev.* **15,** 1419–1426
65. Hirokawa, N. (1998) *Science* **279,** 519–526
66. King, S. M. (2000) *Biochim. Biophys. Acta* **17,** 60–75
67. Jaffrey, S. R., and Snyder, S. H. (1996) *Science* **274,** 774–777

Roles of TRP14, a Thioredoxin-related Protein in Tumor Necrosis Factor-α Signaling Pathways

Woojin Jeong, Tong-Shin Chang, Emily S. Boja, Henry M. Fales and Sue Goo Rhee

J. Biol. Chem. 2004, 279:3151-3159.
doi: 10.1074/jbc.M307959200 originally published online November 7, 2003
